Synergistic effect of aluminum hypophosphite and intumescent flame retardants in polylactide postprint

Authors: Zhou, X, Li, J, Wu, YG

Date: 2017-04-06T00:00:00+00:00

Abstract

Aluminum hypophosphite (AHP) was introduced into polylactide/intumescent flame retardant (PLA/IFR) systems by melt blending. The flame retardant and thermal properties of the PLA composites were investigated. The results suggest that a synergistic effect

Full Text

Preamble

Synergistic Effect of Aluminum Hypophosphite and Intumescent Flame Retardants in Polylactide

Xuan Zhou^{a,b}, Juan Li^{a,*} and Yonggang Wu^{b}

Aluminum hypophosphite (AHP) was introduced into polylactide/intumescent flame retardant (PLA/IFR) systems via melt blending. The flame retardant and thermal properties of the PLA composites were investigated. The results suggest that a synergistic effect exists between IFR and AHP on char formation and anti-dripping behavior of PLA composites. PLA/IFR composites containing 10 wt% IFR can pass the UL-94 V-0 rating, but the test is accompanied by heavy melt dripping. For PLA/AHP, a UL-94 V-2 rating is obtained at the same loading. However, composites containing 7 wt% IFR and 3 wt% AHP pass the UL-94 V-0 rating with modified dripping behavior.

Moreover, the char from combustion of PLA/IFR is flexible but of poor quality, while that for PLA/AHP is brittle with many cracks. In contrast, the char for PLA/IFR/AHP is strong and compact, enabling it to resist erosion from heat and gas formation and protect the interior of the matrix. In addition, AHP causes crosslinking among APP, which promotes char formation and prevents

melt dripping. This is the main reason for the good flame retardant properties of PLA composites.

Keywords: anti-dripping; aluminum hypophosphite; intumescent flame retardant; polylactide; synergism

Introduction

Growing environmental awareness and petroleum resource shortages have prompted the development and application of bio-based and biodegradable polymers. Poly(lactic acid) (PLA) is the first viable thermoplastic that can be produced from plant-based feedstock and processed using conventional melt processing techniques. It is also one of the most important bioplastics and has received considerable attention in recent years due to its excellent properties: biodegradability, availability from abundant renewable sources, and good mechanical and thermal characteristics. However, like other polyester resins, PLA exhibits poor flame retardancy due to its intrinsic chemical composition and molecular structure, limiting its wider applications in automotive interior systems, the electrical industry, and other fields. While the thermal and mechanical properties of PLA have been modified dramatically in recent years, and various commercial materials based on PLA resin have become available for packaging, molding, and other applications, flame retardancy remains a major issue limiting its expanded use.

Many types of flame retardants can be used to modify PLA' s flame retardant properties, with environmentally friendly systems being more competitive. These include phosphorus-containing compounds, nitrogen-based systems, silicones, inorganic fillers, nanoparticles, and IFR systems. Among these, IFR is one of the most promising green candidates due to its excellent properties such as low smoke production, non-toxicity, halogen-free nature, and lack of corrosive gas generation. A typical IFR system contains three components: an acid source, a carbonization agent, and a blowing agent. In traditional IFR systems, ammonium polyphosphate (APP), pentaerythritol (PER), and melamine (MA) act as the acid source, carbonization agent, and blowing agent, respectively.

The effects of traditional and novel IFR systems on PLA' s flame retardant properties have been widely reported. These studies include using natural resources as charring agents, synthesizing IFRs with new structures, copolymerizing or grafting flame retardant elements onto the PLA main chain, introducing catalysts or synergists into the IFR system, and combining multiple types of flame retardants. For example, lignin and starch have been substituted for PER in APP/PER systems, and the resulting PLA composites can pass UL-94 V-0 compared to V-2 for PLA/APP/PER composites. A novel flame retardant, spirocyclic pentaerythritol bisphosphorate diphosphoryl melamine (SPDPM), which integrates acid, char, and gas sources in a single molecule, has been prepared and used in PLA. It was found that SPDPM improves the flame retardancy and anti-dripping performance of PLA, with composites containing 25 wt% SPDPM

achieving UL-94 V-0 rating and a limiting oxygen index (LOI) value of 38.

Based on this background, it might seem that good flame retardant properties for PLA can be obtained easily. However, melt-dripping behavior is difficult to eliminate at low IFR content due to PLA' s intrinsic properties. Melt dripping not only broadens the burning surface area but also increases the intensity of secondary damage during combustion. The dripping behavior of PLA during combustion has been the focus of earlier work. For example, the effects of organic montmorillonite (O-MMT) on the flame retardancy and melt stability of PLA/IFR have been studied, showing that O-MMT can significantly enhance melt stability and suppress melt dripping. It has also been found that some nanofillers such as polyhedral oligomeric silsesquioxane (POSS) and carbon nanotubes lessen the melt-dripping behavior of PLA to some extent, though UL-94 vertical burn properties remain poor. The introduction of 40% calcium sulfate and 3% clay into PLA yields a material that burns without dripping in UL-94 HB tests. The dripping performance of burning PLA can be improved by strengthening char formation, thickening the char layers, or introducing inorganic particles to increase resin viscosity. However, in no case has perfect anti-dripping behavior combined with good flame retardant performance been achieved due to PLA' s good flowability and poor heat resistance.

Clearly, more effective strategies to control dripping during PLA combustion are needed. Hypophosphite salts have been used as components of flame retardant materials, with many organic or inorganic hypophosphite salts prepared and evaluated. The effect of aluminum diethylphosphinate (AlPi) and nanoparticles with different geometries on PLA combustion has been examined, revealing that char residue from PLA/AlPi contains segregated aluminum phosphate microspheres that do not provide a good barrier for gas and heat flow. The thermal degradation of PLA/aluminum hypophosphite (AHP) composites has been investigated, showing that PLA composites containing 20 wt% AHP can pass the UL-94 V-0 test, though the char formed displays a porous surface, suggesting it is brittle and not tough enough to resist heat and gas flow. Combustion of PLA/IFR composites typically produces intumescent char residues that are not very strong and provide poor resistance to heat and gas flow. Combining AHP and IFR might lead to the formation of a compact, non-porous char residue upon PLA combustion, which could be beneficial for achieving good flame retardancy.

In our laboratory, AHP has been introduced into a conventional PLA/IFR system (APP and PER in a 3:1 weight ratio). The PLA/IFR/AHP composites were prepared by melt blending, and their flame retardant and combustion dripping performance were investigated using LOI, UL-94 vertical burn tests, and cone calorimetry. Scanning electron microscopy (SEM) and X-ray photoelectron spectroscopy (XPS) were used to observe the morphology and composition of char residues. Additionally, thermogravimetric analysis (TGA) was employed to investigate the thermal degradation process of the PLA composites.

Experimental Section

Materials

PLA (2002D) was purchased from Nature Works LLC. APP (n > 1000) was provided by Hangzhou JLS Flame Retardant Chemical Company. PER was purchased from Aladdin. AHP was obtained from Wuhan Hanye Chemicals New Material Co., LTD. All materials were dried under reduced pressure at 80°C for 12 h before use.

Preparation of Flame Retardant PLA Composites

The flame retardant PLA composites were prepared using a Brabender mixer at 180°C with a roller speed of 50 rpm for 8 min. After mixing, all samples were hot-pressed at 190°C under 10 MPa for 3 min into sheets with dimensions of 100.0 mm × 100.0 mm × 3.0 mm, then cut into standard sample bars for LOI and UL-94 testing. The formulations of PLA samples are presented in Table 1 .

Measurements

The char formed after LOI testing was first sputter-coated with a conductive layer and then observed using a TM-1000 Tabletop SEM with a 15-kV accelerating voltage.

The molecular weight of PLA was tested by gel permeation chromatography (GPC). Samples were dissolved in chloroform and analyzed on a Waters 1515 gel chromatograph at normal temperature.

Thermal degradation of the samples was examined under N_2 flow using a METTLER TOLEDO TGA/DSC1 Analyzer over a temperature range from 50°C to 800°C with a heating rate of 10°C/min. These experiments were repeated three times, with consistent results; data from one representative run are presented.

An AXIS ULTRADLD Multifunctional X-ray Photoelectron Spectroscope was employed to investigate element migrations and chemical bonds in the char. Specimens were prepared by grinding the char residues in a mortar.

Cone calorimeter measurements were performed using an FTT cone calorimeter according to ISO 5660 standard under a heat flux of 35 kW/m^2. Test sheets measured 100.0 mm × 100.0 mm × 3.0 mm. Each specimen was wrapped in aluminum foil and exposed horizontally. Cone data reported represent the average of three replicated experiments.

LOI values were measured using a 5801 digital oxygen index analyzer (Kunshan Yang Yi Test Instrument Co., Ltd.) according to ASTM D2863-97. Test specimens measured 100.0 mm × 6.5 mm × 3.0 mm.

UL-94 vertical burn tests were performed using an AG5100B vertical burning tester (Zhuhai Angui Testing Equipment Company, China) according to ASTM

D3801. Specimens measured 100.0 mm × 13.0 mm × 3.0 mm. LOI and UL-94 results were repeated three times.

Results and Discussion

Flammability of PLA Composites

The LOI, UL-94 ratings, and dripping behavior of PLA loaded with AHP and IFR are summarized in Table 1. Pure PLA has a low LOI value (21.3) and exhibits heavy dripping during combustion. Introducing 10 wt% AHP into PLA increases the LOI to 25.5 (PLA-1) and modifies the dripping behavior; however, the UL-94 rating is only V-2 due to long flaming times. When AHP content increases to 15 wt%, dripping during the first 10 s of UL-94 testing is eliminated, achieving a V-1 rating (PLA-2), though the LOI value increases only slightly to 26.6.

In contrast, IFR dramatically increases the LOI value. Adding just 10 wt% IFR to PLA yields an LOI of 33.4 and a UL-94 V-0 rating, though combustion is accompanied by heavy dripping. Even with 35 wt% IFR, dripping is not completely eliminated despite an LOI exceeding 50. When both AHP and IFR are present at a total content of 10 wt%, all samples achieve UL-94 V-0 rating. As AHP content increases, LOI decreases slightly. However, as the IFR/AHP ratio changes from 7/3 to 3/7, samples PLA-6, PLA-7, and PLA-8 show no drops during the first ignition in UL-94 testing. Although these samples soften during the second 10 s, the dripping behavior is clearly modified.

Comparing PLA/IFR composites with and without AHP at an IFR/AHP ratio of 7:3 reveals that 30 wt% of a single IFR is required to eliminate dripping during the first 10 s of UL-94 testing—three times the content needed when both AHP and IFR are present. This suggests improved efficiency due to synergistic effects. Interestingly, at total flame retardant contents above 15 wt%, PLA composites containing AHP show higher LOI values than those without AHP, opposite to the trend observed at lower loadings. These results indicate that AHP and IFR exhibit synergistic effects not only on dripping behavior but also on LOI enhancement at higher flame retardant contents. At 35 wt% total flame retardant content, composite PLA-16 achieves UL-94 V-0 rating without dripping or softening during either the first or second 10 s, with a high LOI of 53.9. Related photos after LOI and UL-94 testing are displayed in Figs. 1 and 2 [FIGURE:1][FIGURE:2].

Figure 1 shows photographs of pure PLA and PLA composites after LOI tests. Pure PLA leaves little char residue after combustion. Obvious intumescent char is observed for PLA/AHP composites (PLA-1). Char residue increases slightly with IFR introduction (PLA-3). However, PLA-6 containing both IFR and AHP shows superior char quality and quantity compared to others at the same 10 wt% loading. A significant difference exists between PLA-9 and PLA-10: the former shows a mixture of char and melted resin, while the latter exhibits an intumescent char layer without melted resin, indicating potential anti-dripping

ability. A high-quality, intumescent char can not only restrain heat erosion but also reduce melt dripping, thus imparting good flame retardant properties.

Figure 2 presents photos of PLA and its composites after UL-94 tests. Both PLA-1 and PLA-3 show melt dripping during the first 10 s, with char residue weight causing drops. In contrast, PLA-6 not only forms a char layer but also demonstrates anti-dripping effects compared to PLA-3 and PLA-1 during the first ignition. As flame retardant content increases, melt dripping diminishes. At 35 wt% IFR and AHP content, only the sample top becomes charred, with dripping and softening disappearing completely during both the first and second 10 s, yielding good anti-dripping behavior.

Thermal Degradation of PLA Composites

TGA was used to investigate reactions between IFR, AHP, and PLA. Figure 3

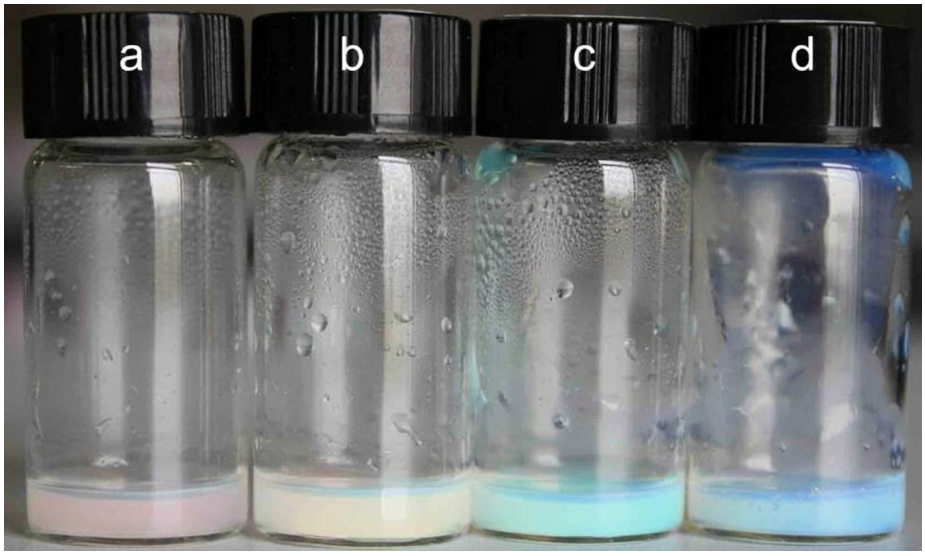

Figure 1: Figure 3

shows experimental (Exp.) and calculated (Cal.) TGA curves for IFR, AHP, and PLA. The Cal. curve was obtained from the TGA curves of individual components based on their mass percentages. In Fig. 3(a), the 1 wt% decomposition temperature (T_1wt%) of IFR is about 200°C, lower than 300°C for AHP. The residue for IFR is 28.7 wt%, much lower than AHP' s 70.2 wt% at 800°C. The Exp. curve T_1wt% for the AHP/IFR mixture is 10°C lower than the Cal. curve, suggesting possible chemical reactions between them. Moreover, the Exp. curve residue at 800°C is 3.5 wt% higher than the Cal. curve, indicating that AHP may accelerate IFR degradation at low temperatures, enabling earlier decomposition and enhanced char formation at higher temperatures.

Figure 3(b) shows Exp. and Cal. curves for PLA/IFR. The Exp. curve has a lower T_1wt% and higher char residue at 800°C than the Cal. curve. IFR degrades at lower temperatures and triggers chemical reactions in PLA at reduced temperatures, helping to form more char and increasing high-temperature residue. Figure 3(c) shows similar results for PLA/AHP: the Exp. T_1wt% is lower than the Cal. value, while char residue at 800°C is higher. These results demonstrate that both IFR and AHP can accelerate PLA degradation at lower temperatures while increasing char residue at higher temperatures. AHP also promotes degradation and char formation in the IFR system, creating dual effects in the PLA/IFR/AHP system.

Thermal stability of pure PLA and various PLA composites under N_2 atmosphere is shown in Fig. 4 [FIGURE:4], with related data listed in Table 2 . PLA-3 possesses the lowest T_2wt% among all samples with the same additive content, indicating that IFR has a greater effect on early thermal degradation of PLA than AHP. The T_2wt% of PLA-6 is about 15°C higher than PLA-3, possibly due to AHP' s good thermal stability and its promotion of crosslinking reactions in IFR. Higher additive content leads to lower T_2wt%; PLA-10' s T_2wt% decreases to 244.0°C at 15 wt% additive content. At higher temperatures, additive effects on degradation temperature become less pronounced—for example, T_{50}wt% values for PLA-0, PLA-1, PLA-3, and PLA-6 are similar. Char residue at 800°C for PLA/AHP is higher than for PLA/IFR at the same additive content, with PLA-6 falling between them. Consequently, IFR shows greater effect on PLA thermal degradation, while AHP plays a more important role in charring behavior. The PLA/IFR/AHP system combines these two effects, generating a synergistic improvement in flame retardant properties.

Figure 5 [FIGURE:5] shows TGA curves of pure PLA and its composites in air atmosphere, with related data in Table 3 . PLA and its composites exhibit secondary degradation after 350°C in air. All PLA composites have lower T_2wt% than pure PLA, though the difference is smaller than in N_2. For example, PLA-1' s T_2wt% is only 1.5°C lower than PLA-0. Moreover, T_5wt% for PLA-1, PLA-3, and PLA-6 remains similar to PLA-0, suggesting poorer additive effects on thermal stability in air versus N_2. However, char residues differ significantly among samples. Pure PLA decomposes completely by 500°C, while PLA-1 and PLA-3 have char residues of 7.7 wt% and 6.1 wt%, respectively. The char layer for PLA-3 is unstable, with its amount decreasing as temperature increases, whereas PLA-1's char residue remains stable, decreasing only slightly from 500°C to 800°C. These results indicate that AHP helps form a stable charring layer that enhances char formation in PLA/IFR. The charring layer from PLA/IFR, rooted in crosslinking reactions between APP and PER, is weak but tough (few cracks observed in char residue as shown in Fig. 7 [FIGURE:7]) and can toughen the char from PLA/AHP. Therefore, compounding IFR and AHP into PLA produces a synergistic effect on flame retardant properties.

Cone Calorimeter Test of PLA Composites

Cone calorimetry is an ideal method for assessing flammability under simulated real fire conditions, providing parameters such as heat release rate (HRR), peak heat release rate (PHRR), total heat release (THR), and residual weight over time. The relationships between these parameters and time for PLA and its composites are shown in Fig. 6 [FIGURE:6], with related data including time to ignition (TTI) and mean mass loss rate (mean MLR) listed in Table 4 .

As shown in Fig. 6a and Table 4, the HRR curve for PLA-0 rises rapidly to PHRR after ignition then decreases quickly. This shape changes upon introducing AHP and IFR. PLA composites containing AHP (PLA-1) show rapid HRR increase but slow decrease. TTI for PLA-1 is 30 s shorter than PLA-0, reaching PHRR in only 100 s. Conversely, TTI for PLA-3 is 23 s longer than PLA-0, and while time to PHRR is extended, PHRR value is not dramatically reduced. This suggests that AHP makes materials more easily ignitable, while IFR hinders ignition. With both flame retardants present, PHRR is lower than PLA-0, with AHP showing more obvious effects. PLA-6' s PHRR drops 54% compared to PLA-0, and HRR decreases slowly over time. At higher flame retardant content (15 wt%), PLA-10 shows lower HRR and PHRR than PLA-6.

THR is commonly used to evaluate fire safety in real fires. As demonstrated in Fig. 6b, PLA-0' s THR is 94.2 MJ/m^2 at 600 s, while PLA-1 and PLA-3 have THR values of 98.1 MJ/m^2 and 116.9 MJ/m^2, respectively, indicating that single AHP or IFR does not reduce PLA' s THR. PLA-6 containing both AHP and IFR has a lower THR of 92.3 MJ/m^2, likely related to the high-quality char layer shown in Fig. 7. PLA-10' s THR decreases to 51.3 MJ/m^2, 42.9 MJ/m^2 lower than PLA-0. Interestingly, composites containing AHP (PLA-1, PLA-6, PLA-10) degrade earlier than PLA-3 with only IFR, differing from TGA results. This discrepancy arises because cone calorimetry simulates real fire conditions while TGA uses programmed temperature ramps under N_2 or air, yielding different results. The flame retardant mechanisms of AHP and IFR in PLA are also different, as discussed below.

Char residue for PLA-0 is only 2.6 wt% after cone calorimeter testing. PLA-1 produces 15.5 wt% char residues at the end of burning, while PLA-3 yields 11.7 wt%. This again demonstrates that AHP benefits crosslinking and char formation reactions. Furthermore, PLA-6 shows the highest char residues (26.3 wt%), 10.8 wt% and 14.6 wt% higher than PLA-1 and PLA-3, respectively. This differs from TGA results where PLA-6' s char residue fell between PLA-1 and PLA-3, indicating that a good synergistic effect on charring behavior occurs when both AHP and IFR are used. The continuous, swollen, dense char formed in PLA-6 effectively protects the matrix from further degradation and provides more opportunities for char formation. While TGA uses only several milligrams, preventing perfect char layer formation, cone calorimeter tests use larger samples where complete char layers can form. Increasing flame retardant content to 15 wt% raises PLA-10' s char residues to 42.6 wt%.

Mean MLR reflects the pyrolysis rate and behavior at selected radiation intensity. Polymers pyrolyze into small volatile molecules during heating; more volatile molecules yield higher mean MLR values and fewer residual solids. Pure PLA has the highest mean MLR among all samples, with values for PLA composites following the trend: PLA-3 > PLA-1 > PLA-6 > PLA-10. This matches PHRR and char residue trends, again proving the synergistic effect between IFR and AHP. This synergistic effect forms a higher quality char layer during combustion, which effectively separates the matrix from heat and oxygen.

Structure and Morphology of Char Residues

Figure 7 [FIGURE:7] presents photographs of char residues after cone calorimeter tests. PLA-0 shows almost no char residue. With flame retardants, obvious charring layers appear for all samples. PLA-1' s char layer is fine and rigid but brittle, forming several cracks and holes during combustion. PLA-3 displays an intumescent, compact char layer, but it is too weak to resist heat and gas erosion, and insufficient char residue creates a large gap in the middle. PLA-6 residues show a compact, tough char layer with no surface cracks, superior to both PLA-1 and PLA-3. This char layer completely covers the resin, preventing burning and degradation. PLA-10 shows a similar char layer to PLA-6 with larger expanded volume. These results suggest that combining AHP and IFR helps form a strong, compact char layer—the main reason for better flame retardant properties in PLA/IFR/AHP composites.

Char residues from different PLA composites after cone testing were observed by SEM, as shown in Fig. 8 [FIGURE:8]. The char layer of PLA-1 consists of charring microparticles packed loosely with holes and gaps, resulting in poor flame retardant performance despite large char amounts. In contrast, PLA-3' s char residue surface is compact and smooth with few holes or cracks. When AHP and IFR are combined, PLA-6 and PLA-10 char layers become compact and smooth, with improved quality and increased quantity. It is speculated that separated char particles from PLA/AHP can be bound by the adhesive char from PLA/IFR, while simultaneously strengthening it. Consequently, the merits of both AHP and IFR are realized, yielding better flame retardant performance.

Chemical components of char residues were investigated using XPS. As shown in Table 5 and Fig. 9 [FIGURE:9], the peak at 284.6 eV corresponds to C H and C C in aliphatic and aromatic species. The peak at 285.8 eV is attributed to C O in C O P and/or C O H. Peaks around 288.6 eV characterize C=O and/or C=N. The peak at 283.4 eV is attributed to Al O C. O1s spectra show bonds from 531.4 to 532.1 eV; peaks around 531.8 eV correspond to =O in phosphate or carbonyl groups, while the peak centered at 532.8–533.1 eV is assigned to O in C O P, C O H, P O P groups and/or absorbed water. N1s spectra show a peak at about 400.5 eV, assigned to N H and/or N O groups. The low N1s concentration in Table 6 indicates low content of related functional groups, as nitrogen typically exists as NH_3 that escapes during combustion. The peak at about 134.3 eV corresponds to P2p from single phosphate, pyrophosphate, and

polyphosphate or their mixtures. Peaks around 75 eV are attributed to Al2p in phosphate and/or pyrophosphate.

Table 6 shows element concentrations. P element in PLA-6 char increases to 17.34 wt% from 9.17 wt% (PLA-1) and 14.43 wt% (PLA-3). O element in PLA-6 char increases to 45.86 wt% from 31.62 wt% (PLA-1) and 37.73 wt% (PLA-3). These results reflect the effects of individual AHP, IFR, and their interaction. As shown in Scheme 1(1–4) and literature [16–19], AHP releases phosphine and produces $Al_2(HPO_4)_3$ upon heating; phosphine can be oxidized to phosphoric acid in the presence of oxygen. At high temperatures, $Al_2(HPO_4)_3$ degrades to aluminum pyrophosphate, releasing water, while phosphoric acid dehydrates to form polyphosphoric acid. IFR works through two pathways: most APP releases NH_3 to form polyphosphate and generate phosphorimidic groups (Scheme 1(5,6)), or APP reacts with PER to release NH_3 and water (Scheme 1(7,8)). Above 280°C, aromatic species consisting of phosphacarbonaceous layers appear and begin forming char until about 550°C. In this system, NH_4^+ in APP can be replaced by Al^{3+}, which may react with three monomeric phosphate groups, releasing three NH_3 molecules and creating a crosslinking point among three APP chains (Scheme 1(9,10)). This crosslinking stabilizes APP and decreases phosphorus oxide volatility during pyrolysis, making more phosphorus available for phosphorylation and char formation. The AHP/IFR combination induces formation of a strong, compact char layer that acts as a good barrier, preventing phosphine gas escape and retaining more P in the condensed phase. Notably, N content in PLA-6 char residues exceeds that in PLA-3, despite PLA-6 having only 70% of PLA-3' s nitrogen source (IFR). Since nitrogen from APP mainly evolves as NH_3 gas during hydroxyl condensation reactions between APP and PER or during polymerization (Scheme 1(5–8)), self-polymerization of APP produces more NH_3 and H_2O, leaving less nitrogen in the condensed phase. This indicates that AHP promotes reactions between APP and PER. Furthermore, the better char layer in PLA-6 hinders oxygen penetration into the melted resin, creating a barrier that slows APP self-polymerization, thereby retaining more nitrogen in char residues. The increased P and N content facilitates formation of high-quality charring layers, producing a good synergistic effect and flame retardant properties.

PLA is a very sensitive polymer, and AHP can degrade the host matrix due to its instability at high temperatures. If molecular weight decreases, dripping is promoted during UL-94 testing. Therefore, PLA molecular weight before and after processing was tested by GPC, as shown in Table 7 . Processing significantly affects PLA molecular weight, decreasing it from 1.78×10^5 to 1.39×10^5 due to thermal degradation alone. Introduction of AHP (PLA-1) and IFR (PLA-3) also decreases molecular weight, but less severely than thermal degradation. PLA is more sensitive to IFR than AHP. Thus, flame retardants in PLA not only modify flammability but also promote degradation during processing, making performance a composite result of multiple actions.

Based on these results, the synergistic mechanism between AHP and IFR is

concluded as follows. First, char induced by AHP is brittle and disconnected, while that from IFR is flexible but poor. IFR benefits LOI increase, while AHP helps hinder melt dripping and achieve good UL-94 ratings. Only the combination of both flame retardants can form a good char layer. Second, IFR facilitates substrate crosslinking and char layer evolution, but IFR decomposition produces nonflammable H_2O and NH_3 gases that promote PLA degradation, causing PLA-3 to decompose earlier than PLA-0 and PLA-1 in TGA tests. In cone calorimeter tests, however, the bulk material produces nonflammable gases quickly, making PLA-3's TTI longer than PLA-0 and PLA-1. Additionally, char formation speed in PLA/IFR is insufficient, allowing some melting resin to mix with formed char during combustion, as shown in LOI testing. Conversely, AHP has good thermal stability, releasing PH_3 that oxidizes to phosphoric acid in the presence of oxygen, which then generates polyphosphoric acid through dehydration. Such acids promote matrix dehydration, crosslinking, and char formation, increasing char residue amounts. These residues enhance the IFR-formed char layer and hinder resin melting. Third, incombustible gases from IFR cause rapid char layer expansion, while AHP facilitates APP crosslinking, both preventing melt dripping and increasing P content in PLA-6. Good flame retardant properties are thus achieved. Excess AHP causes LOI decrease, so a suitable AHP/IFR ratio is necessary for optimal flame retardancy in the PLA/AHP/IFR system.

Conclusions

AHP was introduced into the PLA/IFR system to enhance flame retardant properties. A good synergistic effect on char formation and anti-dripping behavior was found between AHP and IFR, resulting in better flame retardant performance. PLA composites with 7 wt% IFR and 3 wt% AHP can pass UL-94 V-0 rating with modified dripping behavior. Char formed by PLA/IFR is flexible but poor, while that from PLA/AHP is brittle with many cracks. In contrast, char from PLA composites containing both IFR and AHP is strong and compact, exceeding that of composites with separate IFR or AHP. Charring particles induced by AHP enhance the char layer derived from IFR in the PLA system, while the IFR-derived char binds these microparticles together. This creates a good char layer that resists heat and gas erosion, better protecting the interior matrix. It also helps prevent volatile combustion gases from escaping, providing more opportunities for char formation. AHP promotes crosslinking among APP, beneficial for reducing melt dripping and retaining more P and N in char residues. Consequently, more components remain in the condensed phase, forming high-quality charring layers that impart good flame retardancy to PLA.

Acknowledgements

This work was financially supported by the National Natural Science Foundation of China (nos. 21274159 and 51473178) and the Program for Ningbo Innovative Research Team (Grant 2009B21008). The authors declare no competing

financial interest.

References

[1] L. T. Sin, A. R. Rahmat, W. A. Rahman, *Polylactic acid: PLA biopolymer technology and applications*. Access Online via Elsevier, Oxford, 2012.

[2] C. Reti, M. Casetta, S. Duquesne, S. Bourbigot, R. Delobel, Polym. Adv. Technol. 2008, 19(6), 628-635.

[3] J. Zhan, L. Song, S. B. Nie, Y. Hu, Polym. Degrad. Stab. 2009, 94(3),

[4] L. L. Wei, D. Y. Wang, H. B. Chen, L. Chen, X. L. Wang, Y. Z. Wang, Polym. Degrad. Stab. 2011, 96(9), 1557-1561.

[5] K. Tao, J. Li, L. Xu, X. L. Zhao, L. X. Xue, X. Y. Fan, Q. Yan, Polym. Degrad. Stab. 2011, 96(7), 1248-1254.

[6] D. Y. Wang, Y. P. Song, L. Lin, X. L. Wang; Y. Z. Wang, Polymer 2011, 52(2), 233-238.

[7] X. Y. Yuan, D. Y. Wang, L. Chen, X. L. Wang, Y. Z. Wang, Polym. Degrad. Stab. 2011, 96(9), 1669-1675.

[8] X. Q. Liu, D. Y. Wang, X. L. Wang, L. Chen, Y. Z. Wang, Polym. Degrad. Stab. 2011, 96(5), 771-777.

[9] S. M. Li, H. Yuan, T. Yu, W. Z. Yuan, J. Ren, Polym. Adv. Technol. 2009, 20(12), 1114-1120.

[10] K. Fukushima, M. Murariu, G. Camino, P. Dubois, Polym. Degrad. Stab. 2010, 95(6), 1063-1076.

[11] C. X. Zhao, Y. Liu, D. Y. Wang, D. L. Wang, Y. Z. Wang, Polym. Degrad. Stab. 2008, 93(7), 1323-1331.

[12] G. Tang, R. Zhang, X. Wang, B. B. Wang, L. Song, Y. Hu, X. L. Gong, J. Macromol. Sci. A 2013, 50(2), 255-269.

[13] C. H. Ke, J. Li, K. Y. Fang, Q. L. Zhu, J. Zhu, Q. Yan, Y. Z. Wang, Polym. Degrad. Stab. 2010, 95(5), 763-770.

[14] S. Bourbigot, S. Duquesne, G. Fontaine, S. Bellayer, T. Turf, F. Samyn, Mol. Cryst. Liq. Cryst. 2008, 486, 1367-1381.

[15] M. Murariu, L. Bonnaud, P. Yoann, G. Fontaine, S. Bourbigot, P. Dubois, Polym. Degrad. Stab. 2010, 95(3), 374-381.

[16] N. A. Isitman, M. Dogan, E. Bayramli, C. Kaynak, Polym. Degrad. Stab. 2012, 97(8), 1285-1296.

[17] G. Tang, X. Wang, W. Y. Xing, P. Zhang, B. B. Wang, N. N. Hong, W. Yang, Y. Hu, L. Song, Ind. Eng. Chem. Res. 2012, 51(37), 12009-12016.

[18] K. C. Cheng, C. B. Yu, W. Guo, S. F. Wang, T. H. Chuang, Y. H. Lin, Carbohyd. Polym. 2012, 87(2), 1119–1123.

[19] Y. Kiuchi, M. Iji, T. Yanagisawa, T. Shukichi, Polym. Degrad. Stab. 2014, 109(11), 336–342.

[20] G. Tang, X. Wang, R. Zhang, B. B. Wang, N. N. Hong, Y. Hu, L. Song, X. L. Gong, Ind. Eng. Chem. Res. 2013, 52, 7362–7372.

[21] S. Bourbigot, M. LeBras, R. Delobel, L. Gengembre, Appl. Surf. Sci. 1997, 120(1–2), 15–29.

[22] Q. He, H. Lu, L. Song, Y. Hu, L. Chen, J. Fire Sci. 2009, 27(4), 303–321.

[23] J. F. Moudler, W. F. Stickle, P. E. Sobol, K. D. Bomben, *Handbook of X-ray photoelectron spectroscopy*. Perkin-Elmer, Eden Prairie, MN, 1992, 52.

[24] A. F. Grand, C. A. Wilkie, *Fire retardancy of polymeric materials*. CRC Press, Florida, 2000, 803, 217–43.

[25] H. F. Zhu, J. Li, Y. K. Zhu, S. J. Chen, Polym. Adv. Technol. 2014, 25(8),

[26] M. Lewin, M. Endo, Polym. Adv. Technol. 2003, 14, 3–11.